



HAL
open science

Progress in edge plasma turbulence modelling hierarchy of models from 2D transport application to 3D fluid simulations in realistic tokamak geometry

H. Bufferand, J. Bucalossi, G. Ciruolo, G. Falchetto, A. Gallo, Ph. Ghendrih, N. Rivals, P. Tamain, H. Yang, G. Giorgiani, et al.

► **To cite this version:**

H. Bufferand, J. Bucalossi, G. Ciruolo, G. Falchetto, A. Gallo, et al.. Progress in edge plasma turbulence modelling hierarchy of models from 2D transport application to 3D fluid simulations in realistic tokamak geometry. Nuclear Fusion, 2021, 61 (11), pp.116052. 10.1088/1741-4326/ac2873 . hal-03377162

HAL Id: hal-03377162

<https://hal.science/hal-03377162>

Submitted on 14 Oct 2021

HAL is a multi-disciplinary open access archive for the deposit and dissemination of scientific research documents, whether they are published or not. The documents may come from teaching and research institutions in France or abroad, or from public or private research centers.

L'archive ouverte pluridisciplinaire **HAL**, est destinée au dépôt et à la diffusion de documents scientifiques de niveau recherche, publiés ou non, émanant des établissements d'enseignement et de recherche français ou étrangers, des laboratoires publics ou privés.



Distributed under a Creative Commons Attribution - NonCommercial - NoDerivatives 4.0 International License

Progress in edge plasma turbulence modelling hierarchy of models from 2D transport application to 3D fluid simulations in realistic tokamak geometry

**H. Bufferand, J. Bucalossi, G. Ciruolo, G. Falchetto, A. Gallo,
Ph. Ghendrih, N. Rivals, P. Tamain, H. Yang and the WEST
team**

IRFM-CEA, F-13108 Saint-Paul-Lez-Durance, France

E-mail: hugo.bufferand@cea.fr

G. Giorgiani, F. Schwander, M. Scotto d'Abusco, E. Serre

Aix-Marseille Univ., CNRS, Centrale Marseille, M2P2, Marseille, France

Y. Marandet, M. Raghunathan

Aix-Marseille Univ., CNRS, PIIM, Marseille, France

JET team

see the author list of E. Joffrin et al. 2019 Nucl. Fusion 59 112021

Abstract.

This contribution presents the recent effort at CEA and French federation for Fusion to simulate edge plasma transport with the new code SOLEDGE3X. The latter can be used both as a 2D transport code or as a 3D turbulence code. It makes possible simulating edge plasma up to the first wall including the complex wall geometry. It also includes neutral recycling and impurity sputtering, seeding and transport. In order to improve turbulence description in transport simulation, a reduced model for turbulence intensity prediction has been derived and implemented, based on “k-epsilon” like models from the neutral fluid community. Applications to a JET L-mode detached plasma and to a WEST plasma are used as illustration of the code abilities

Submitted to: *Nucl. Fusion*

1. Introduction

Accurate modelling of cross-field turbulent transport in tokamaks edge plasma remains a challenge, many key experimental features such as edge transport barriers formation

being still hard to simulate, especially for ITER size tokamaks. Being able to predict the SOL width or the power load imbalance between inner and outer divertor legs even for today's JET size tokamaks is still an open issue. First principle modelling of edge plasma turbulence is thus today a very active topic in the fusion community driving many dedicated research projects such as the TSVV European boundary code project in Europe.

Despite this effort towards first principle modelling of the turbulent transport, 2D transport codes where the cross-field turbulent transport is emulated by ad-hoc diffusion remain today the most popular tool for experiments analysis or engineering applications. In these codes, the prescription of the diffusion coefficients rely on empirical basis and are usually adjusted to match simulation and experimental at a given location (usually mid-plane profiles). In this empirical procedure, the nature of the turbulence behind these transport coefficients is most of the time not taken into account. The main drawback of this approach is to lack predictability by missing the basic physics of turbulence mechanisms.

In order to address both the first principle modelling of edge turbulence but also to feed information about turbulence into transport codes, a dedicated effort has been made at IRFM in the last two years to develop the new code SOLEDGE3X presented in Section 2 which aims at encompassing a hierarchy of models from standard 2D transport code to 3D first principle turbulence modelling. The development of this new code comes from the merging of the transport code SOLEDGE2D [1] and the turbulence code TOKAM3X [2] previously developed within the French fusion community. Integrating features of the two latter codes, SOLEDGE3X is able to simulate tokamak edge plasma either in 2D or 3D, including: the realistic wall geometry, neutrals since it is coupled to EIRENE and impurities since the code is fully multi-species, based on the state-of-the-art Zhdanov collisional closure for multi-component plasmas. First results of turbulent plasma in WEST geometry including the sputtering of the wall have been produced in 2019 and represent a major step for first principle modelling of tokamak plasma in realistic conditions.

However, since full 3D simulations remain expensive in CPU time, it is still profitable to use SOLEDGE3X as a transport code in 2D to run fast interpretative simulations. Section 3 presents an original idea implemented in SOLEDGE3X to improve turbulent transport predictability and go beyond the standard empirical approach is to use a reduced model for turbulence in the same fashion as the “k-epsilon” widely used in neutral fluid community. One or two equations are added to the standard mass, momentum and energy balance to describe the evolution of the turbulence intensity k and optionally the evolution of the turbulence dissipation ε . This model is used as a platform to include some ingredients of the turbulence physics - such as the interchange instability in the framework of 2D transport codes. Of course, this reduced model is not first principle and require an empirical closure. We use the multi-machine scaling law for the SOL width λ_q to do so, as a first approach of data assimilation. When SOLEDGE3X is used as a transport code with this reduced “k-

epsilon” model for turbulence activated, the number of free parameters is drastically reduced since there is no need to prescribe transport coefficients, the “k-epsilon” model predicting a 2D map of cross-field diffusivities. Since the model is based on interchange instability, one recovers for instance the ballooning of radial transport in the low field side mid-plane. Also, since the model is closed using the multi-machine scaling law, the overall level of transport is automatically adjusted to get a SOL width compatible with this scaling law. This closure with the scaling law is thus powerful to obtain reasonable profiles, however it is also a weakness of the model since in principle, one could not reproduce an experiment where the SOL width does not follow the scaling law. This is the drawback of this kind of semi-empirical models which are not first principle and thus limited by the main assumptions behind their closure. In order to test the applicability of this reduced model for turbulence, a series of L-mode TCV shots have been simulated and the simulation results have been compared with experimental data. Even if the simulation does not recover exactly the SOL width measured in the experiment, the overall agreement in term of peak heat flux, density and temperature on the target is quite remarkable. This “k-epsilon” model has shown to be a promising first step toward integration of turbulence physics inside transport simulations.

To go further, the advantage of the SOLEDGE3X code is to be able to run also first principle turbulent simulations where the turbulence intensity can be directly measured, see Section 4. The comparison between turbulent simulations and the reduced model for turbulence should in the future provide a clear path to improve these reduced models for turbulence. In that perspective, first results of full turbulent simulation in TCV like geometry should help interpreting the results obtained with the reduced “k-epsilon” model and identify missing ingredients.

2. The SOLEDGE3X code

Developed from the merging of the codes SOLEDGE2D and TOKAM3X developed at IRFM, the new code SOLEDGE3X implements a fluid description of the edge plasma based on the drift-fluid approximation. Braginskii like equations can be solved either in 2D or in 3D. The 2D simulations can be used for two different purposes: Firstly, the code can be used as a transport code (similar to SOLPS-ITER [3] for instance); in this case, a symmetry is assumed (e.g toroidal symmetry for a tokamak or symmetry around the magnetic axis for a linear machine) and the turbulent cross-field transport is emulated using anomalous diffusivities. Secondly, the code can be used as a 2D turbulent code (similar to HESEL [4] for instance) assuming flute approximation [5]. The code can also be used in 3D. It can then be used for two purposes: as a 3D transport code, for instance including non-symmetric wall elements like antenna limiters or as a 3D turbulence code or as a 3D turbulent code (similar to GBS [6], STORM [7] or GRILLIX [8]) modelling both the turbulent structure micro-scales and the large-scale plasma flows.

2.1. The drift-fluid model implemented in SOLEDGE3X

Despite the different nature of the above-mentioned set-up, the code always solves the same system of equations: a mass balance, a parallel momentum balance and an energy balance for every charged species. In addition, the current balance is solved to compute the electric potential. In its present version, the code is electrostatic and the magnetic field is fixed and taken as an input of the code. The set of equations is summarized as follow: for all charged species:

$$\partial_t n + \vec{\nabla} \cdot (n\vec{v}) = S_n \quad (1)$$

$$\begin{aligned} \partial_t(mnv_{\parallel}) + \vec{\nabla} \cdot (mnv_{\parallel}\vec{v}) = & -\nabla_{\parallel} p + ZnE_{\parallel} \quad (2) \\ & + \vec{\nabla} \cdot \left(\nu_{\parallel} \nabla_{\parallel} v_{\parallel} \vec{b} + mn\nu_{\perp} \vec{\nabla}_{\perp} v_{\parallel} \right) + S_{v_{\parallel}} \end{aligned}$$

$$\begin{aligned} \partial_t \mathcal{E} + \vec{\nabla} \cdot (\mathcal{E}\vec{v}) = & -\vec{\nabla} \cdot (pv_{\parallel}\vec{b}) + Zn\nu_{\parallel} E_{\parallel} \quad (3) \\ & + \vec{\nabla} \cdot \left(\nu_{\parallel} v_{\parallel} \nabla_{\parallel} v_{\parallel} \vec{b} + mn\nu_{\perp} v_{\parallel} \vec{\nabla}_{\perp} v_{\parallel} \right) \\ & + \vec{\nabla} \cdot \left(\kappa_{\parallel} \nabla_{\parallel} T \vec{b} + h_{\parallel} \vec{b} + \chi_{\perp} n \vec{\nabla}_{\perp} T \right) + v_{\parallel} R_{\parallel} + Q + S_{\mathcal{E}} \end{aligned}$$

Where n is the species density; \vec{v} the species velocity (1st order in the drift ordering) that is decomposed as a parallel velocity v_{\parallel} , “E cross B” drift $\vec{v}_E = \vec{E} \times \vec{B}/B^2$ where $\vec{E} = -\vec{\nabla}\phi$ denotes the electric field, diamagnetic drift $\vec{v}^* = -\vec{\nabla}p \times \vec{B}/ZnB^2$ and anomalous diffusive transport $\vec{v}_D = -D_{\perp} \vec{\nabla}_{\perp} n/n$. m denotes the species mass and Z the species charge number. The species temperature T is used to compute species pressure $p = nT$ and species total energy $\mathcal{E} = \frac{3}{2}nT + \frac{1}{2}mnv_{\parallel}^2$. Parallel viscosity ν_{\parallel} , parallel heat conductivity κ_{\parallel} , parallel friction force in between species R_{\parallel} , parallel heat flux due to inter-species collisions h_{\parallel} and energy equipartition term Q take values computed by Zhdanov collisional closure for multi-component plasmas [5, 9, 10, 11]. For a simple hydrogenic plasma, Braginskii's closure can also be used. Source terms S_n , $S(v_{\parallel})$ and $S_{\mathcal{E}}$ gather ionisation-recombination-radiation sources as well as external sources such as additional power deposit by heating systems. Finally, cross-field diffusivities D_{\perp} , ν_{\perp} and χ_{\perp} can either take classical value ($\sim 10^{-2}m^2s^{-1}$) for turbulent simulations or “anomalous” value ($\sim 1m^2s^{-1}$) for transport simulations, the cross-field diffusion then emulating turbulent transport. For electrons, only the energy equation is solved, the electron density being computed assuming quasi-neutrality and electron velocity being computed assuming ambipolarity. The current balance is solved in addition to the above set of equations:

$$\vec{\nabla} \cdot \left(j_{\parallel} \vec{b} + \vec{j}^* + \vec{j}_{pola} + \vec{j}_{diff} \right) = 0 \quad (4)$$

Where j_{\parallel} is the parallel current given by the generalised Ohms law:

$$j_{\parallel} = -\sigma_{\parallel} \left(\nabla_{\parallel} \phi + \frac{\nabla_{\parallel} p_e}{n_e} - \frac{R_{\parallel, T_e}}{n_e} \right) \quad (5)$$

The diamagnetic current \vec{j}^* is computed as $\vec{j}^* = \sum_{e,i} Zn\vec{v}^*$ whereas the polarisation current is computed similarly (neglecting electron polarisation velocity) $\vec{j}_{pola} =$

$\sum_i Z n \vec{v}_{pola}$. The polarisation velocity is a second order velocity in the drift ordering that takes a quite complex expression:

$$\vec{v}_{pola} = -\frac{1}{n} \left(\partial_i \vec{\omega} + \vec{\nabla} \cdot (\vec{v} \otimes \vec{\omega}) \right) \quad (6)$$

where

$$\vec{\omega} = \frac{m}{Z B^2} \left(n \vec{\nabla} \phi + \frac{1}{Z} \vec{\nabla} p \right) \quad (7)$$

One can define the vorticity $\Omega = \vec{\nabla} \cdot \sum_i Z \vec{\omega}$, homogeneous to a charge. The current equation hence takes the form of a vorticity equation

$$\partial_t \Omega + \vec{\nabla} \cdot \left(\sum_i Z \vec{\nabla} \cdot (\vec{v} \otimes \vec{\omega}) \right) = \vec{\nabla} \cdot \left(j_{\parallel} \vec{b} + \vec{j}^* + \zeta \vec{\nabla}_{\perp} \Omega \right) \quad (8)$$

The diffusion current being used to regularise the expression $\vec{j}_{diff} = \zeta \vec{\nabla} \Omega$.

2.2. Boundary conditions

SOLEGE3X uses finite volumes numerical scheme to solve the above cited mass, momentum, energy and current balances. The grid is structured and aligned with magnetic flux surfaces and cannot thus be also aligned with the wall. To deal with complex wall geometries, the grid is extended inside the wall and a mask function determines which points are in the plasma and which points are in the wall. Figure 1 shows an example of boundary condition mask for a JET case. Wall boundary conditions are applied on faces where the transition between points in the plasma and points in the wall. The following boundary conditions inspired by Bohm-Chodura boundary conditions apply there:

- Outgoing velocity normal to the wall greater that parallel sound speed normal to the wall:

$$|\vec{v} \cdot \vec{n}_{wall}| \geq |c_s \vec{b} \cdot \vec{n}_{wall}| \quad (9)$$

This property guarantees that the total plasma velocity is oriented outward

- Sheath transmission factor between energy and particle fluxes:

$$\phi_{\mathcal{E},se} = \left(\gamma T + \frac{1}{2} m v_{\parallel}^2 \right) \phi_{n,se} \quad (10)$$

Where for each species, $\phi_{\mathcal{E},se}$ is the total energy flux at sheath entrance, $\phi_{n,se}$ is the particle flux at sheath entrance and γ is the sheath transmission factor about 2.5 for ions and 4.5 for electrons.

- Total plasma current on the wall is given by

$$j_{wall} = \left(1 - \exp \left(\Lambda - \frac{\phi}{T_e} \right) \right) \sum_i Z \phi_{n,se} \quad (11)$$

Where the ions saturation current is computed from ions particle fluxes $\sum_i Z \phi_{n,se}$ and where Λ denotes the normalised potential drop in the sheath $\Lambda \sim 3$.

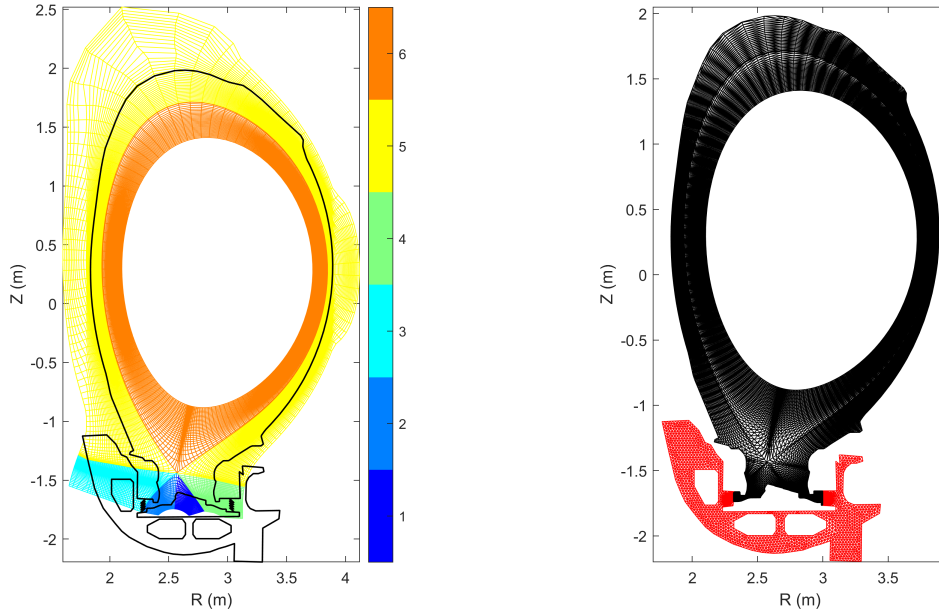


Figure 1. Left: Example of domain decomposition for a JET case (single X-point configuration). Right: EIRENE grid used for neutrals. In black, triangles where plasma is computed - in red, triangles without plasma background (subdivertor).

2.3. Numerical implementation

SOLEEDGE3X relies on a finite volumes numerical scheme. Divergences in every grid point are computed integrating fluxes on the faces of grid elements. The grid is structured and aligned with magnetic surfaces. A domain decomposition is used to treat X-point topology, see Figure 1 for a JET case where 6 domains are used to deal with the X-point. The following numerical methods are used to compute fluxes:

- Advection: 3rd order WENO interpolation and Donat, Marquina fluxes for modified Riemann solver [12]
- Parallel diffusion: since the grid is aligned with magnetic flux surfaces, the parallel diffusion can be solved independently for each flux surface. For 2D cases, the parallel diffusion can be treated as N_{FS} (number of flux surfaces) 1D problems aligned with the grid: simple 2nd order finite differences are used. For 3D cases, the parallel diffusion becomes N_{FS} 2D problems. The grid is no longer aligned with parallel diffusion which occur across both the poloidal and toroidal direction. Günter scheme [13] is used to avoid numerical diffusion in this case.
- Perpendicular diffusion: perpendicular diffusion couples all the points of the domain. We use preserving monotonicity scheme for anisotropic diffusion [14].

The implementation of the different operators has been verified using the method of manufactured solution [11].

Most of operators are treated explicitly in time. Only parallel diffusion which has the fastest dynamic is treated implicitly for mass, momentum and energy balances. The current equation takes a different form as other equation. The electric potential being the unknown, it can be rewritten schematically $\partial_t \Delta_{\perp} \phi + \Delta_{\parallel} \phi = RHS$ where the time derivative applies to the perpendicular Laplacian of the unknown. This perpendicular Laplacian must then also be solved implicitly. The matrix used to write the electric potential equation hence couples all the points of the domain. Besides, the anisotropy between a fast dynamic in the parallel direction and a slower one in the perpendicular direction makes the matrix ill-conditioned. If direct solvers such as PASTIX [15] can be used for small 2D cases, they become too time consuming for 3D cases. The best approach found so far relies on iterative solvers, more precisely algebraic multigrid preconditioner followed by Krylov solvers (GMRES or BiCGstab). Different libraries have been coupled to the code such as AGMG [16], PETSC-GAMG [17], or HYPRE-BoomerAMG [18].

2.4. Neutrals

The code SOLEDGE3X implements two neutral models:

- A crude fluid model for neutrals where neutrals transport is considered diffusive. Despite its simplicity, this model provides a good approximation for the source of plasma generated by recycling as well as power losses by radiation in the divertor. It is used mainly for turbulent simulations where the detail of neutral transport is not yet necessary and where a gross estimation of the sources is enough for the scoping studies
- A full kinetic description of neutrals including complex neutrals chemistry. This is done by a coupling of SOLEDGE3X with the neutral Monte-Carlo code EIRENE [19] widely used in the community. A grid based on triangles is used for neutrals, see Fig 1. Interpolations between the SOLEDGE3X quadrangles and the EIRENE triangles are done within the SOLEDGE3X-EIRENE interface, preserving mass and energy conservation.

3. k-epsilon model for turbulence prediction in transport mode

For experiments interpretation and for the preparation of future tokamaks operation, two-dimensional transport simulations remain very popular for integrating a broad range of physical aspects of the plasma wall interaction, from plasma recycling, wall sputtering to impurity transport. They are also quite fast to compute and make possible parameter scans for a reasonable computing time. However, the main drawback is the poor description of the cross-field transport since the plasma turbulent structure cannot be simulated assuming toroidal symmetry. In the mean field approach, the turbulent transport is emulated by an effective diffusion process of mass, momentum and energy, the ad-hoc diffusivities being to be determined most of the time empirically. In the

diffusive assumption, the transport becomes local since the flux is determined only by the local gradient. Turbulence measurements and simulations show that turbulent structures can however propagate ballistically over a long range which may contradict the local approximation made in the diffusive assumption. Several contributions have proposed non-local formulations [20] to go beyond diffusion and the subject is still open. Another key missing ingredient in the mean field approach is by definition the fluctuations. In the averaging procedure of transport equations, several non-linearities are neglected, see the example below for ionization cross-section for instance:

$$S_n = n_n n_e \langle \sigma v \rangle_{iz}(T_e) \quad (12)$$

Averaging gives:

$$\overline{S_n} = n_n \overline{n_e} \overline{\langle \sigma v \rangle_{iz}(T_e)} + n_n \widetilde{n_e} \widetilde{\langle \sigma v \rangle_{iz}(T_e)} \quad (13)$$

Most of the time, in mean field codes, the second term is neglected and the non-linearity of the ionisation cross-section is neglected giving:

$$\overline{S_n} = n_n \overline{n_e} \langle \sigma v \rangle_{iz}(\overline{T_e}) \quad (14)$$

The impact of the excursion of plasma parameters around their average due to fluctuation can be taken into account to compute “fluctuation dressed” cross-section for instance, see [21, 22]. However, to use these expressions in practice in a transport code, one needs at least to estimate the level of fluctuations in the plasma.

In order to feed some information about turbulence in mean field transport simulations, a heuristic turbulence model inspired from the “k-epsilon” model used in neutral fluid community has been implemented in SOLEDGE3X. It relies either on a single equation describing the production, saturation and transport of the turbulence intensity $k \sim \tilde{v}_E^2 [m^2 s^{-2}]$ or a coupled system of two equations describing the evolution of the turbulence intensity k and of its dissipation rate ε . The second model enables in principle a richer description of turbulence properties, see [23, 24]. Other models have been proposed in the community with one or two equations, see [25, 26]. The field is still very open to find an efficient model for turbulence enabling a better predictability for cross-field transport in transport codes, going beyond the state-of-the-art empirical setting of cross field diffusivities. We present in this contribution the simplest model, the single k equation implemented in SOLEDGE3X. Despite its simplicity, this model computes self-consistently a map of diffusion coefficients. The latter is computed from k as $D = \tau k$ where the time τ is taken as $\tau = R/c_s$. In addition to the diffusion coefficient, the model also provides an estimation of the fluctuation level in the plasma enabling the use of “fluctuation dressed” cross sections (though not yet tested in SOLEDGE3X so far). The equation for k is the following:

$$\partial_t k + \vec{\nabla} \cdot (k \vec{v}) = S_k - P_k + \vec{\nabla} \cdot (D \vec{\nabla}_\perp k) \quad (15)$$

Where S_k denotes the source of turbulence and P_k a saturation mechanism for turbulence intensity. Interchange instability has been considered as the main source of turbulence

and thus the linear growth rate of interchange instability is used to compute S_k :

$$S_k = \gamma_I k = c_s \sqrt{\max\left(\frac{\vec{\nabla} p}{p} \cdot \frac{\vec{\nabla} B}{B}, 0\right)} k \quad (16)$$

The saturation of turbulence remains a free parameter in the model. We chose it to be quadratic hence $P_k = \alpha k^2$. We decided to close it from experiments, ensuring that the model recovers experimental scaling laws for the SOL width. More precisely, neglecting transport terms in the k equation, at steady state source and saturation terms must compensate each other giving $S_k = P_k$ hence $k = \gamma_I/\alpha$. Given the expression $D = Rk/c_s$, and the theoretical SOL width for a diffusive model with Bohm boundary conditions at the target: $\lambda_{SOL}^2 = DL_{\parallel}/c_s^2$, one gets $\lambda_{SOL}^2 = \frac{2\pi q R^2}{c_s^2} \times \frac{\gamma_I}{\alpha}$. If one wants the system to recover $\lambda_{SOL} = \lambda_{scaling}$, the parameter α takes the value $\alpha = \gamma_I \left(\frac{2\pi q R^2}{c_s^2}\right) \frac{1}{\lambda_{scaling}^2}$. For L-mode plasma, we usually consider the simple scaling law $\lambda_{scaling} = 4q\rho_L$, the parameter α can then be rewritten as $\alpha = \gamma_I \frac{1}{c_s^2} \frac{\pi A^2}{8q\rho^* r^2}$.

The model has been applied with success to TCV L-mode discharges [23]. Below is presented an example of application to a JET detached plasma from the M18-27 ‘‘Isotope effects on detachment in L-mode’’ experiment. The experimental set-up is summarized in Figure 2. The magnetic equilibrium used corresponds to JET shot #95235. This shot is a density ramp in L-mode with a fixed 1MW NBI heating during the ramp and an Ohmic power in the range of 2MW.

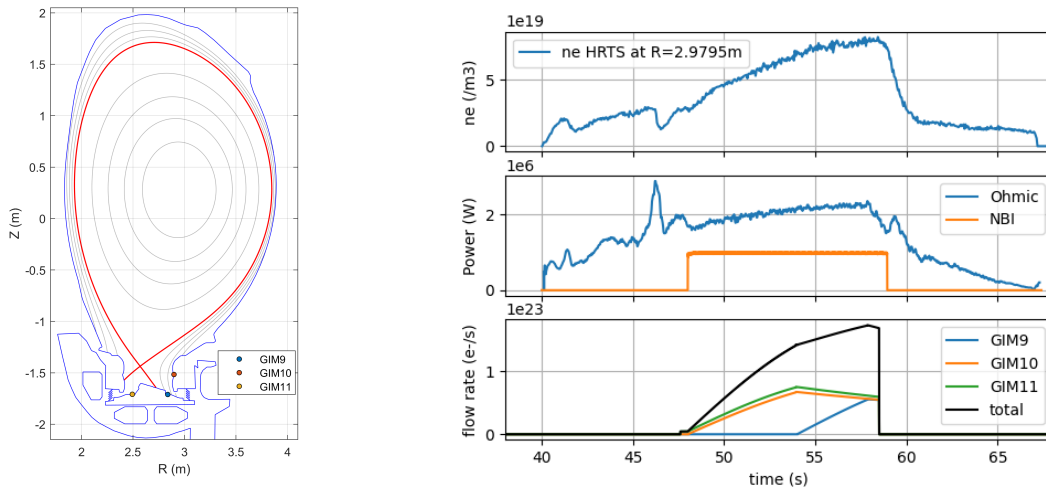


Figure 2. Left: magnetic equilibrium for JET #95235 at $t = 54s$. Gas injection locations are shown. Right: Time traces of core density, power and gas injection during the discharge

A SOLEDGE3X simulation is run with the following parameters trying to match experimental settings at $t = 54s$: 3MW of power are injected about $r/a \approx 0.85$ with a 50/50 repartition between ions and electrons. The recycling coefficient is set to 0.99 on the Beryllium part of the JET wall and 1 on the Tungsten part. The recycling coefficient

on the cryopump surface is set to 0.5. Concerning the particle fuelling, gas is injected from GIM10 and GIM11 locations and the puff rate is automatically adjusted to match a plasma density equal to $3.5 \cdot 10^{19} m^{-3}$ at the separatrix. No transport coefficients are prescribed since their values are computed by the k-model.

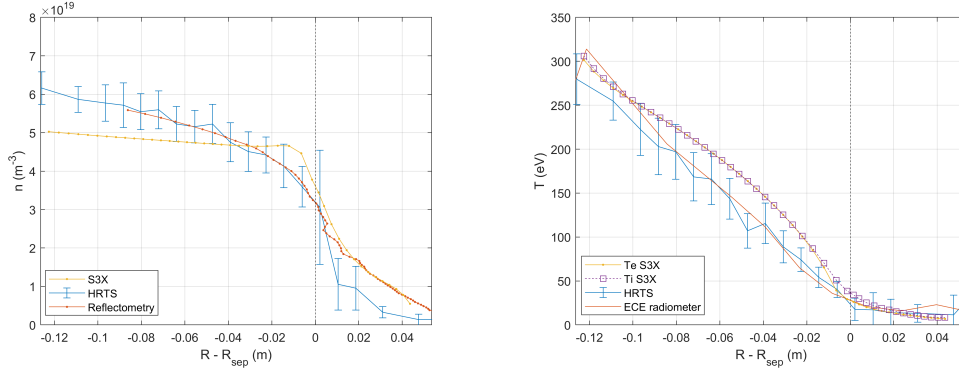


Figure 3. Comparison between midplane profiles computed by SOLEDGE3X-EIRENE and measured on JET

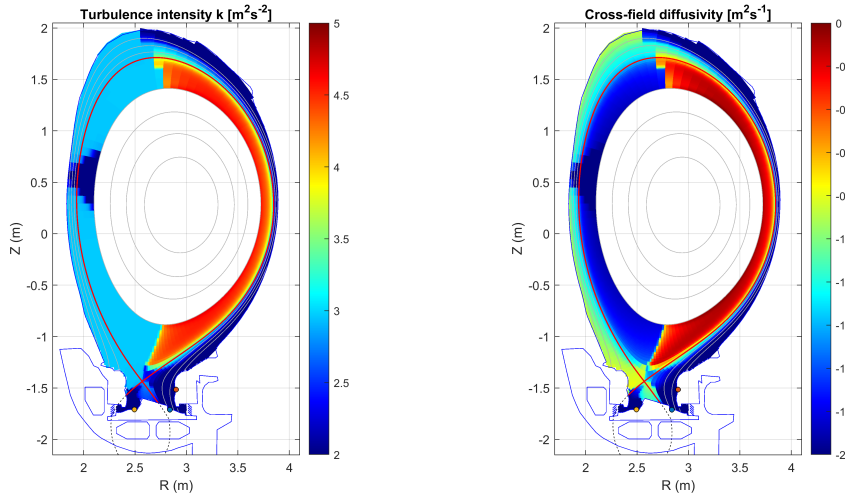


Figure 4. Poloidal map of turbulence intensity k (left) and subsequent cross-field diffusivity D (right) computed by the reduced model

Figure 3 shows a comparison between simulation results and experimental measurements. The overall gradients are well recovered by the k-epsilon model. Figure 4 shows quantities computed by the reduced turbulence model. One recovers a ballooning of the turbulence intensity on the low field side. Turbulence propagates on the high field side by parallel transport.

Figure 5 compares radiation location between simulation and experimental tomographic reconstruction. The radiation seems more concentrated around the X-point in the simulation compared to the experimental radiation map. This may be due

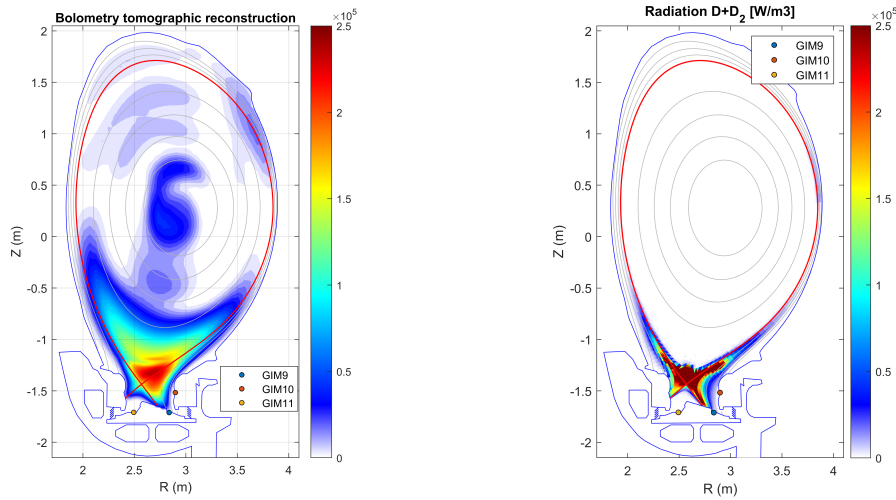


Figure 5. Comparison between radiation map computed by SOLEDGE3X-EIRENE and tomographic reconstruction from bolometry. The strong density gradients near the separatrix are explained by the presence of a strong particle source around the X-point, confirmed by X-point radiation

to the absence of radiating impurities in the simulation. Also, the density peaking in the closed flux surface region is not caught by the simulation. A radial pinch might be needed to recover this feature.

4. Full 3D turbulent simulations in X-point geometry

In addition to its ability to emulate turbulence in a 2D transport mode, either with ad-hoc diffusivities or with reduced models for turbulence, the SOLEDGE3X code is able to perform full 3D turbulent simulations including the main ingredients of the plasma-wall interactions such as recycling or wall sputtering. Here is an illustration of 3D simulation of the WEST tokamak, including the complex wall geometry of WEST. The diffusive neutral model is used to simulate plasma recycling. The size of the machine and the intensity of the magnetic field have been reduced for numerical reasons, the resolution needed for a real scale WEST simulation being out of reach of the code today. Figure 6 shows simulation results, in particular the nice plasma filaments propagating on the tokamak low-field side.

Wall sputtering by the plasma filaments has also been taken into account once again using the simple diffusive model for the neutral sputtered species (in this case, despite the wall is in Tungsten, we chose to sputter Carbon as a proxy for the light impurities trapped at the surface of the tungsten such as oxides, Carbon co-deposits...). One notices that despite its simplicity, the fluid neutral model generates plasma sources at the right location and with a reasonable intensity. It is thus a good candidate to start implementing neutral physics in edge plasma turbulent simulations and it has been implemented in other codes such as GRILLIX [27].

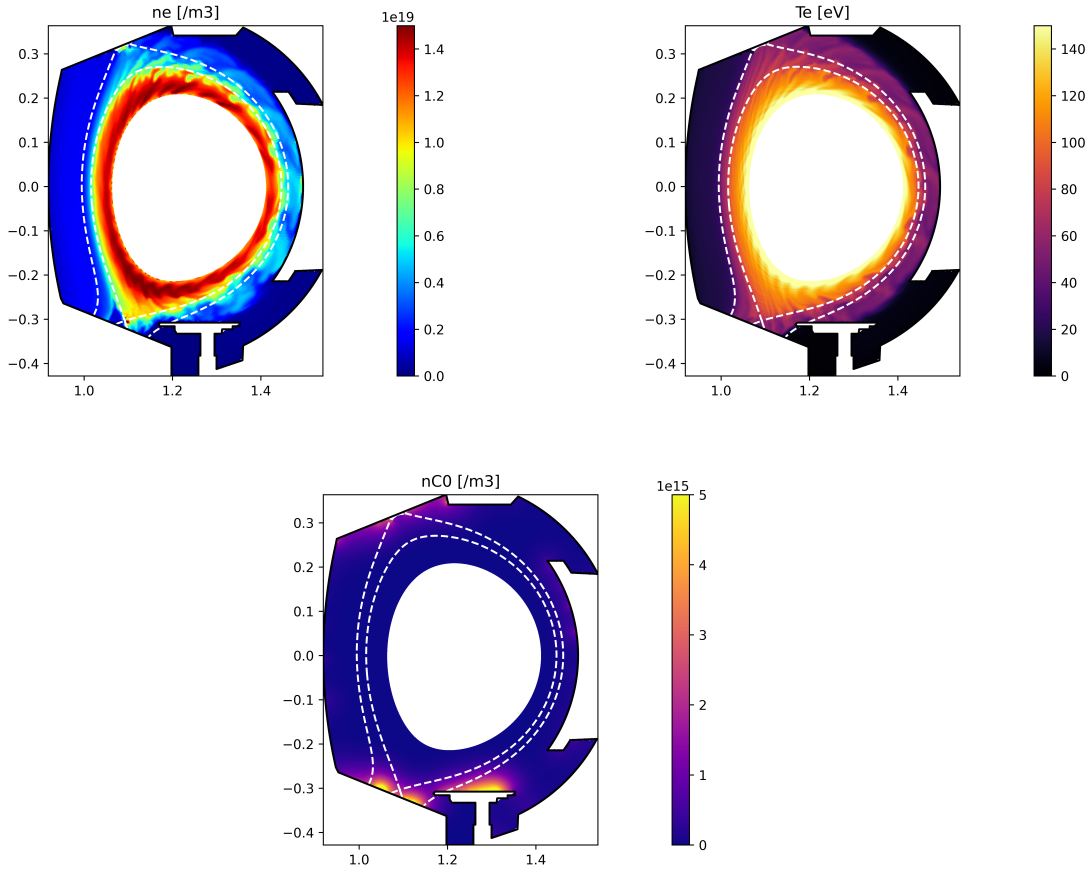


Figure 6. SOLEDGE3X simulation results for a 3D WEST case including recycling and Carbon sputtering. Top left: electron temperature. Top right: electron density. Bottom: Carbon neutral density.

5. Conclusions

The new SOLEDGE3X code has been developed in the past few years for a versatile use both as a transport code and as a turbulence code including complex wall geometry, neutrals and impurities. Reduced model for an enhanced prediction of turbulent transport have been implemented, based on “k-epsilon” like models from the neutral fluid community. First results applied to JET and to WEST have been shown in this contribution. A dedicated effort will be made in the near future to improve numerical efficiency of the code, in particular to speed-up the inversion of the electric potential equation which remains the bottleneck in term of computation workload.

Acknowledgements

This work was granted access to the HPC resources of CINES, under the allocation 2020-A0080510482 made by GENCI and to the HPC resources of Aix-Marseille University financed by the project Equip@Meso (ANR-10-EQPX-29-01). This work

was supported by the EoCoE-II project, grant agreement 824158, funded within the EUs H2020 program. This work has been carried out within the framework of the EUROfusion Consortium and has received funding from the Euratom research and training programme 2014-2018 and 2019-2020 under grant agreement No 633053. The views and opinions expressed herein do not necessarily reflect those of the European Commission

6. Bibliography

- [1] H. Bufferand *et al.* Numerical modelling for divertor design of west device with a focus on plasma-wall interactions. *Nucl. Fusion*, 55, 2015.
- [2] P. Tamain *et al.* The tokam3x code for the edge turbulence fluid simulations of tokamak plasmas in versatile magnetic geometries. *J. Comp. Phys.*, 321, 2016.
- [3] S. Wiesen *et al.* The new solps-iter code package. *J. Nucl. Mat.*, 463, 2015.
- [4] A.H. Nielsen *et al.* Simulation of transition dynamics to high confinement in fusion plasmas. *Physics Letter A*, 379, 2015.
- [5] H. Bufferand *et al.* Three-dimensional modelling of edge multi-component plasma taking into account realistic wall geometry. *Nucl. Mat. Energy*, 2019.
- [6] F.D. Halpern *et al.* The gbs code for tokamak scrape-off layer simulations. *J. Comp. Phys.*, 315, 2016.
- [7] J. Riva *et al.* Three-dimensional plasma edge turbulence simulations of the mega ampere spherical tokamak and comparison with experimental measurements. *Plasma Phys. Control. Fusion*, 61, 2019.
- [8] A. Stegmeir *et al.* Grillix: a 3d turbulence code based on the flux-coordinate independent approach. *Plasma Phys. Control. Fusion*, 60, 2018.
- [9] V. M. Zhdanov. *Transport Processes in Multicomponent Plasma*. Taylor & Francis, 2002.
- [10] M. Raghunathan *et al.* Generalized collisional fluid theory for multi-component, multi-temperature plasma using the linearized Boltzmann collision operator for scrape-off layer/edge applications. *Plasma Phys. Control. Fusion*, 63, 2021.
- [11] H. Bufferand *et al.* Implementation of multi-component zhdanov closure in soledge3x (pre-print). *HAL hal-03243371, v1*, 2021.
- [12] R. Donat and A. Marquina. Capturing shock reflections: An improved flux formula. *J. Comp. Phys.*, 125, 1996.
- [13] S. Günter, Q. Yu, J. Krüger, and K. Lackner. Modelling of heat transport in magnetised plasmas using non-aligned coordinates. *J. Comp. Phys.*, 209, 2005.
- [14] P. Sharma and G. Hammett. Preserving monotonicity in anisotropic diffusion. *J. Comp. Phys.*, 227, 2007.
- [15] Gitlab of the pastix library. <https://gitlab.inria.fr/solverstack/pastix>. Accessed: 2021.
- [16] Agmg webpage. <http://www.agmg.eu>. Accessed: 2021.
- [17] Portable, extensible toolkit for scientific computation website. <https://www.mcs.anl.gov/petsc>. Accessed: 2021.
- [18] Scalable linear solvers and multigrid methods website. <https://computing.llnl.gov/projects/hypre-scalable-linear-solvers-multigrid-methods>. Accessed: 2021.
- [19] Eirene website. <http://www.eirene.de>. Accessed: 2021.
- [20] G. Dif-Pradalier *et al.* On the validity of the local diffusive paradigm in turbulent plasma transport. *Phys. Rev. E*, 82, 2010.
- [21] F. Guzman *et al.* Ionization balance of impurities in turbulent scrape-off layer plasmas i: local ionization-recombination equilibrium. *Plasma Phys. Control. Fusion*, 57, 2015.
- [22] Y. Marandet *et al.* Assessment of the effects of scrape-off layer fluctuations on first wall sputtering with the tokam-2d turbulence code. *Plasma Phys. Control. Fusion*, 58, 2016.

- [23] S. Baschetti *et al.* A k-epsilon model for plasma anomalous transport in tokamaks: closure via the scaling of the global confinement. *Nucl. Mat. Energy*, 19, 2019.
- [24] Ph. Ghendrih *et al.* Self-consistent cross-field transport model for core and edge plasma transport. *Hal* - <https://hal.archives-ouvertes.fr/hal-03081473>, 2021.
- [25] R. De Wolf *et al.* Bayesian approach to parameter estimation and model validation for nuclear fusion reactor mean-field edge turbulence modelling. *Nucl. Fusion*, 61, 2021.
- [26] R. Coosemans *et al.* Bayesian analysis of turbulent transport coefficients in 2d interchange dominated exb turbulence involving flow shear. *J. Phys.: Conf. Ser.*, 1785, 2021.
- [27] W. Zholobenko *et al.* Simulations of turbulence, its suppression and profile evolution across the edge and scrape-off layer of asdex upgrade tokamak. *Nucl. Fus.*, 2021 - (IAEA FEC 2020 special issue).